JOURNAL OF SOLID STATE CHEMISTRY **132,** 131–138 (1997)
ARTICLE NO. SC977431

Thermochemistry of Fluoride Perovskites: Heat Capacity, Enthalpy of Formation, and Phase Transition of $NaMgF_3$

L. Topor,* A. Navrotsky,* Y. Zhao,†,[1] and D. J. Weidner†

*Center for High Pressure Research and Department of Geosciences, Princeton University, Princeton, New Jersey 08544; and
† Center for High Pressure Research and Mineral Physics Institute, Department of Earth and Space Sciences, SUNY, Stony Brook, New York 11794

Received October 18, 1996; in revised form April 11, 1997; accepted April 14, 1997

The enthalpies of formation, heat content, heat capacity, and transition of $NaMgF_3$ perovskite have been determined. A new high temperature calorimetric methodology has been applied for the enthalpy of formation measurements. The heat content and heat of formation measurements were done using a "hybrid calorimeter" built recently in our laboratory. For the heat capacity measurements, a Netzsch 404 high-temperature differential scanning calorimeter (DSC) has been used. The enthalpy of formation from the binary fluorides at 298 K is -15.76 ± 2.46 kJ/mol, and that from the elements is -1716.51 ± 2.8 kJ/mol. The measured heat capacities between 313 and 1153 K show a λ-anomaly with a transition at 1051 K. The presence of one peak supports a recent X-ray study which concluded that the crystal structure transforms from the orthorhombic *Pbnm* phase directly to the cubic *Pm3m* phase. The enthalpy of transformation is 2.3 ± 0.03 kJ/mol. The heat content values measured by transposed temperature drop calorimetry are in agreement with those calculated by graphical integration of the experimental heat capacity data obtained by DSC.

INTRODUCTION

Fluoride perovskites of $A^+B^{2+}F_3$ type form a large family of compounds. Thermochemical data for these are scarce compared to data for oxide perovskites of the $A^{2+}B^{4+}O_3$ charge type. A systematic thermochemical study of fluoride perovskites will contribute to a better understanding of structure–stability relations of these and other materials with perovskite-related structures.

From the geophysical point of view, $NaMgF_3$ is of interest because it is isostructural and isoelectronic to $MgSiO_3$ perovskite, which is believed to be the dominant phase in the earth's lower mantle (1). Structural phase transitions in $NaMgF_3$ may provide clues to possible transitions in $MgSiO_3$ perovskite.

[1] Present address: Los Alamos Neutron Science Center, Los Alamos National Laboratory, Los Alamos, NM 87545.

The unprecedented development of high T_c superconductor research has revealed several families of superconductor compounds with a large variety of layered perovskite-related structures similar to fluoride perovskites (2). Knowledge of perovskite systematics may help place these superconductors in a broader context.

The potential application of fluoride mixtures in the space program to provide electric power from solar thermal energy has been investigated recently (3). The heat storage is based on the enthalpy associated with solid to liquid transformation. Multicomponent fluoride mixtures with a high enthalpy of transformation per unit mass appear to be ideal latent thermal storage materials (4, 5).

Because of the importance of fluoride perovskites in applications such as those above, and to extend fundamental understanding of solid state energetics, we have undertaken a study of both the enthalpy of formation and the structural phase transitions in these materials. In this paper we report the enthalpy of formation, heat content, heat capacity, and enthalpy of transition of $NaMgF_3$ perovskite. This study also presents a new high temperature calorimetric methodology for heat of formation measurements.

Earlier investigation of $NaMgF_3$ by X-ray power diffraction (6) showed the progressive structural phase transition on heating, for orthorhombic to tetragonal at 1033 K, and to cubic at 1173 K (the last transition temperature had a large uncertainity of $\pm$ 25 K). The authors discussed this transition in terms of tilting of regular octahedra in a structure where the bonding is largely ionic. There are other perovskites in which regular octahedra are tilted, for example, rare earth orthoferrites $LnFeO_3$ (7), $MgSiO_3$ (8), $CaTiO_3$ (9, 10), and $SrZiO_3$ (11, 12). The conclusions of a recent study of $NaMgF_3$ perovskite by high temperature X-ray powder diffraction (13, 14) are different from the earlier work and will be discussed in more detail later. Thus another goal of the present study is to clarify the phase transition sequence in terms of heat capacity anomalies, to correlate any excess heat capacity with changes in the X-ray patterns indicative of changes in octahedral tilting, and

0022-4596/97 $25.00

to attempt to apply order-parameter formalisms to the structural and thermodynamic data.

EXPERIMENTAL TECHNIQUE AND SAMPLE CHARACTERIZATION

Sample Preparation

NaF 99.98% and MgF_2 99.99% (Morton Thiokol) were used. The fluorides, dried in vacuum at 673 K for 2 h, were used to prepare the mechanical mixtures and to synthesize $NaMgF_3$ perovskite. $NaMgF_3$ was synthesized following the method described by Chao *et al.* (6) and recently used by Zhao *et al.* (13). Stoichiometric proportions of NaF and MgF_2 were ground in an agate mortar and then sintered at 1023 K in air for 5 h. X-ray power diffraction patterns were obtained with a Scintag PAD V automated diffractometer using monochromatic Cu$K\alpha_1$ radiation. The X-ray powder patterns agreed with published powder patterns for $NaMgF_3$ perovskite (neighborite) (6).

For calorimetric study of the enthalpy of formation, two kinds of compositionally equivalent pellets were prepared: mechanical mixture of 65 mol% NaF and 35 mol% MgF_2 and mechanical mixture of 30 mol% NaF and 35 mol% $NaMgF_2$. The mechanical mixtures were ground and mixed for 5 min in a vibrating mill and then pressed into pellets of 22–54 mg and stored in a drying furnace at 393 K. Prior to their drop into the calorimeter the pellets were kept in a desiccator for about 10 min and then weighed. In our calorimetric measurements we used two different $NaMgF_3$ perovskite samples, one prepared at Stony Brook and the other at Princeton. They gave identical results.

General Calorimetric Technique

Calorimetry of fluorides encounters potential problems which may be more severe than those for oxides. These include voltatility of the fluoride, possible reaction with oxygen and/or moisture, and greater difficulty in finding a proper thermodynamic cycle for determining heat of formation. The methods used here have been tailored bearing these points in mind.

Two calorimeters were used in this work. A Netzsch 404 high-temperature differential scanning calorimeter (DSC) has been used to measure the heat capacity, with a heating rate of 20 K/min under flowing argon atmosphere. The following runs were performed: two consecutive heating scans for two $NaMgF_3$ samples (53.46 mg and 59.50 mg), three heating cycles for the empty cell corresponding to "blanks," and three heating cycles for the standard α-Al_2O_3 (corundum, Johnson Mattey, 99.99%) calcined at 1773 K prior to the runs to ensure phase purity. The data were collected at intervals of 2 points per K. The empty cell run data were subtracted from the outputs of the sample scan runs. The results were converted to heat capacities using a calibration factor obtained as a ratio of the α-Al_2O_3 experimental values and the heat capacities reported by NBS (15). The temperature calibration was determined by the manufacturer from the melting points of several metals in the temperature range of operation. An accuracy of 1.5% was obtained by measuring the heat capacity of silica glass over a wider temperature range (313–1673 K).

The heat content and heat of formation measurements (see below) were done using a "hybrid calorimeter," built recently in our laboratory and described previously (16). This calorimeter combines the advantages of the Calvet twin and Setaram HT-1500 calorimeters. The samples (pellets) were dropped from room temperature into an alumina calorimetric crucible which was lined with a platinum crucible. The measurements were done under flowing argon. Data acquisition was by an IBM compatible PC with a National Instrument IEEE-488 interface board (GPIB). Calibration has been achieved with 200- to 300-mg pieces of platinum and showed a standard deviation of about 1%. For heat of formation measurements, the calorimeter was operated at 1273 K. To measure heat content, H_T–H_{298}, various temperatures, especially in the vicinity of the phase transition, were used.

Thermodynamic Cycle for Enthalpy of Formation

Two types of calorimetric methods are generally used for heat of formation measurements. The first is direct reaction (recombination) calorimetry, in which the desired compound is synthesized directly during the calorimetric experiment. Though useful for alloys and intermetallic compounds (17, 18), it is generally inapplicable to ternary oxides and fluorides because they form too slowly. The second class of experiments can broadly be called solution calorimetry: reactants (binary compounds) and products (ternary compounds) are each converted to the same final stage, generally dissolved species either in aqueous acid or in a molten salt solvent. The advantages of high temperature oxide melt solution calorimetry, different oxide melts used as solvents and the requirements which must be satisfied by these solvents have been reviewed by Navrotsky (19, 38). In high temperature oxide melt solution calorimetry the enthalpy of formation is obtained from the heat of solution of the compound and of its component oxides. The solvent commonly used for oxide minerals, $2PbO \cdot B_2O_3$ near 973 K, has been used for some phases containing both oxygen and fluorine (20), but the rates of solution of pure fluorides appear somewhat slow, and the final state of F^- (dissolved in the oxide melt, interacting with cations such as Al or Si, or evolved into the gas phase) has not been fully characterized. To avoid these problems, we developed a new method relying on pure fluorides only and producing a reproducible molten final state.

The enthalpy of formation of $NaMgF_3$ perovskite has been obtained form the heat effects associated with the formation of a liquid mixture of the same composition from the two solid fluoride components ($NaF + MgF_2$) and from the ($NaMgF_3 + NaF$) solid mixture. Two types of pellets have been dropped from room temperature into the calorimeter at 1273 K: a mechanical mixture of NaF and MgF_2 and a mechanical mixture of NaF and $NaMgF_3$. In both cases, the overall composition was 65 mol% NaF and 35 mol% MgF_2, which is near the eutectic between NaF and $NaMgF_3$ (21). The lower liquidus temperature at this composition (~1250 K as compared to a melting point of 1303 K for $NaMgF_3$) ensured rapid mixing and formation of homogeneous liquid in the calorimeter.

This composition can also be expressed as having $NaMgF_3$ and excess NaF in a molar ratio of 1 : 0.8571. On this basis, namely per mole of $NaMgF_3$, the drop of the mechanical mixture of NaF and MgF_2 is represented by the following reaction:

$$1.8571\ \mathrm{NaF} \times \mathrm{l}(298) + \mathrm{MgF_2} \times \mathrm{l}(298) = (1.8571\ \mathrm{NaF} + \mathrm{MgF_2})\ (\mathrm{liq}, 1273). \quad [1]$$

The drop of the second type of pellet, a mixture of NaF and $NaMgF_3$, is represented by

$$0.8571\ (\mathrm{NaF} \times \mathrm{l}(298) + \mathrm{NaMgF_3} \times \mathrm{l}(298) = (1.8571\ \mathrm{NaF} + \mathrm{MgF_2})\ (\mathrm{liq}, 1273). \quad [2]$$

Since final state is the same in both types of experiments, the difference between these two reactions gives

$$\mathrm{NaF} \times \mathrm{l}(298) + \mathrm{MgF_2} \times \mathrm{l}(298) = \mathrm{NaMgF_3} \times \mathrm{l}(298), \quad [3]$$

with $\Delta H_3 = \Delta H_1 - \Delta H_2$. ΔH_3 is thus the enthalpy of formation of $NaMgF_3$ from NaF and MgF_2 at room temperature.

This approach has several advantages over conventional oxide melt solution calorimetry. (1) Because the system contains only fluorides, one need not be concerned about fluoride–oxide interactions. (2) By mixing the $NaMgF_3$ with NaF, a decrease of melting temperature occurs which allows rapid mixing and the formation of a homogeneous liquid without stirring. (3) The enthalpy of formation at 298 K is obtained directly. No heat content correction is necessary. (4) Each drop is a "mini-mixing" experiment forming a liquid mixture with the same composition. The number of drops is not limited by the solubility in the solvent or by change in composition of the melted mixture but only by the volume of the calorimetric crucible. Thus six drops into the same crucible can be made before the crucible is removed. (5) The method is flexible and can be tailored to other ternary fluorides as well as to other systems by varying calorimeter temperature and the composition of the mixture. (6) Because small pellets are used, a small-volume calorimeter can be used. Because the compound of interest is present at high concentrations (30–50 mol%) rather than in a dilute solution (<1 mol%), using small pellets maintains high enough sensitivity. Thus this method is more easily adapted to higher calorimeter temperatures needed for very refractory materials, temperatures at which a conventional lead borate or alkali borate solvent would have too high a vapor pressure. We have recently used a somewhat analogous method for the determination of heat of formation of ternary nitrides (22).

RESULTS AND DISCUSSION

The results of the two types of drop experiments corresponding to Eqs. [1] and [2] are summarized in Tables 1 and 2. The enthalpy of formation from the fluorides is the difference between the two measured enthalpies and is -15.76 ± 2.46 kJ/mol, where the uncertainty results from the propogated errors listed in the tables.

The first published value of the enthalpy of formation of $NaMgF_3$ was an estimate of -32.2 kJ/mol (23). This value was utilized by Holm *et al.* together with other data, in a thermodynamic cycle to calculate the enthalpy of mixing in the system NaF–MgF_2 (21). Later the enthalpy of mixing was measured by Hong and Kleppa (24) and was compared with the earlier result of Holm *et al.* They found inconsistency between the two values which was attributed to an inadequate enthalpy of formation value. This conclusion led

TABLE 1
Transposed Temperature Drop Calorimetry of NaF and MgF_2 Mixture

mg mixture	Joules observed	ΔH (kJ/mol)[a]
43.18	79.82	259.33
35.75	66.85	262.34
42.38	78.06	258.40
37.58	70.57	263.45
35.57	66.25	261.30
41.30	76.64	260.34
33.67	62.50	260.42
25.94	48.52	262.41
38.88	71.88	259.37
29.67	55.23	261.15
36.92	68.04	258.54
	Average	260.64 ± 1.00[b]

[a] Calculated for mixture containing the equivalent of one mole of MgF_2 and 1.8571 mol of NaF, producing a melt with $NaF/(NaF + MgF_2) = 0.65$, as discussed in text.

[b] Error is two standard deviations of the mean.

TABLE 2
Transposed Temperature Drop Calorimetry of NaF and $NaMgF_3$ Mixture

Amount of mixture (mg)	Joules Observed	ΔH(kJ/mol)[a]
54.06	107.08	277.91
39.69	77.89	275.33
26.91	53.06	276.64
37.89	76.13	281.88
30.16	58.43	271.89
28.47	55.03	271.18
24.90	49.67	278.74
37.28	74.26	279.46
36.83	73.33	279.33
31.01	59.85	270.77
33.73	67.51	280.79
22.15	43.09	272.92
	Average	276.40 ± 2.25[b]

[a] Calculated for mixture containing one mole of $NaMgF_3$ and 0.8571 mol of NaF, producing a melt with $NaF/(NaF + MgF_2) = 0.65$, as discussed in text.

[b] Error is two standard deviations of the mean.

TABLE 3
Experimental Heat Capacities of $NaMgF_3$ Perovskite

Temp (K)	C_p (J/mol·K)	Temp (K)	C_p (J/mol·K)	Temp (K)	C_p (J/mol·K)
313.15	106.34	623.15	131.89	933.15	146.10
323.15	108.40	633.15	132.33	943.15	147.00
333.15	111.37	643.15	132.76	953.15	147.96
343.15	113.54	653.15	133.17	963.15	148.98
353.15	115.28	663.15	133.57	973.15	150.08
363.15	116.58	673.15	133.96	983.15	151.39
373.15	117.68	683.15	134.36	993.15	152.82
383.15	118.67	693.15	134.75	1003.15	154.50
393.15	119.55	703.15	135.13	1008.15	155.58
403.15	120.35	713.15	135.52	1013.15	156.78
413.15	121.07	723.15	135.89	1018.15	158.18
423.15	121.73	733.15	136.27	1023.15	160.02
433.15	122.35	743.15	136.64	1028.15	162.29
443.15	122.94	753.15	137.04	1033.15	164.93
453.15	123.50	763.15	137.44	1038.15	168.33
463.15	124.04	773.15	137.83	1043.15	172.45
473.15	124.57	783.15	138.21	1048.15	179.49
483.15	125.10	793.15	138.60	1053.15	214.64
493.15	125.62	803.15	138.98	1058.15	169.87
503.15	126.12	813.15	139.39	1063.15	151.33
513.15	126.61	823.15	139.79	1068.15	146.12
523.15	127.09	833.15	140.20	1073.15	145.05
533.15	127.59	843.15	140.62	1083.15	143.54
543.15	128.08	853.15	141.05	1093.15	143.13
553.15	128.57	863.15	141.49	1103.15	142.79
563.15	129.07	873.15	141.94	1113.15	142.50
573.15	129.57	883.15	142.45	1123.15	142.74
583.15	130.09	893.15	143.02	1133.15	142.07
593.15	130.50	903.15	143.74	1143.15	141.95
603.15	130.97	913.15	144.47	1153.15	141.96
613.15	131.44	923.15	145.26		

the latter authors to measure the enthalpy of formation. Solid–liquid mixing calorimetry was applied by dropping solid MgF_2 in liquid NaF at 1354 K. Correction for the heat content and enthalpy of fusion was applied to obtain the enthalpy of formation at 298 K. The value reported is -16.7 kJ/mol, in good agreement with our value -15.76 ± 2.46 kJ/mol. Converting our value to elemental reference states (25) gives an enthalpy of formation from the elements at 298 K of -1716.51 ± 2.8 kJ/mol.

The heat capacities between 313 and 1153 K obtained by DSC are reported in Table 3 and plotted as a function of temperature in Fig. 1. Each value is an average of four experimental runs with 1.2% the average standard deviation. A λ-anomaly is observed which excludes the possibility of a first-order transition. The transformation temperature obtained as extrapolated onset temperature is 1051 K. The presence of one peak in the C_p-temperature curve and the large heat capacity tail toward low temperature support the recent X-ray study (13, 14) which concluded that the crystal structure transforms from an orthorhombic *Pbnm* phase directly to the cubic *Pm3m* phase. The experimental observations show that the variation of the orthorhombic unit cell dimensions started at 873 K and then the cell "rapidly converge to the cubic Pm3m cell in the temperature interval 873 K–1038 K" (13, 14). This conclusion contradicts that of Chao *et al.* (6), who indicated that a sequence of structural phase transitions take place from orthorhombic to tetragonal at 1033 K and to cubic at 1173 K. The recent X-ray study (13, 14) does not exclude the possibility of transformation from orthorhombic to tetragonal to cubic in a very small temperature interval (1–2 K) below the transition temperature, but due to the temperature fluctuation of ± 2 K in the temperature range 1033–1043 K any such transformation could not be detected. The DSC study does not indicate two peaks but if there is an intermediate tetragonal phase transition within 2–5 K of the observed peak, the two phase transition peaks can overlap. The experimental heat capacity values below the transition have been fitted with an equation of the form recommended by Haas and Fisher (26) without the eT^2 term. This equation has been found satisfactory for reproducing experimental data from room temperature to high temperature (27, 28) and we did not use it for extrapolation at higher temperature where the transformation occurs. The resulting equation is

$$C_p = -22.7894 + 0.084121T + 2938.919T^{-0.5} - 608.2153 \times 10^4 T^{-2} \quad \text{(suitable at 313 to 903 K).} \qquad [4]$$

The absolute average deviation (AAD) of the experimental C_p data from the fitted values is 0.2%. The heat content from 298 to 903 K was calculated by extrapolation

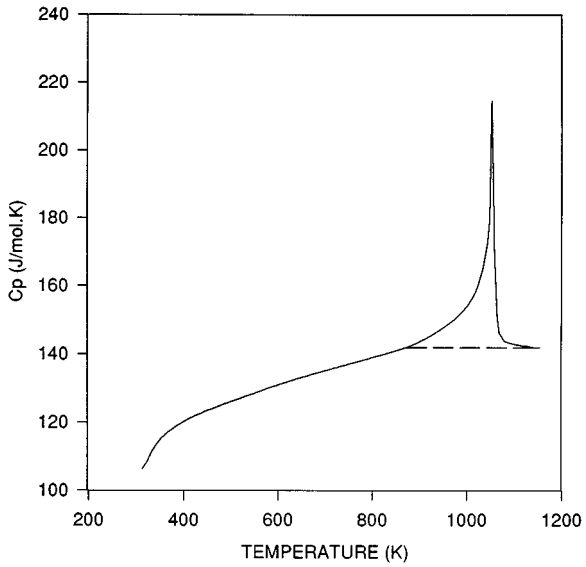

FIG. 1. Measured heat capacity vs temperature. Dotted line represents the baseline, (see text).

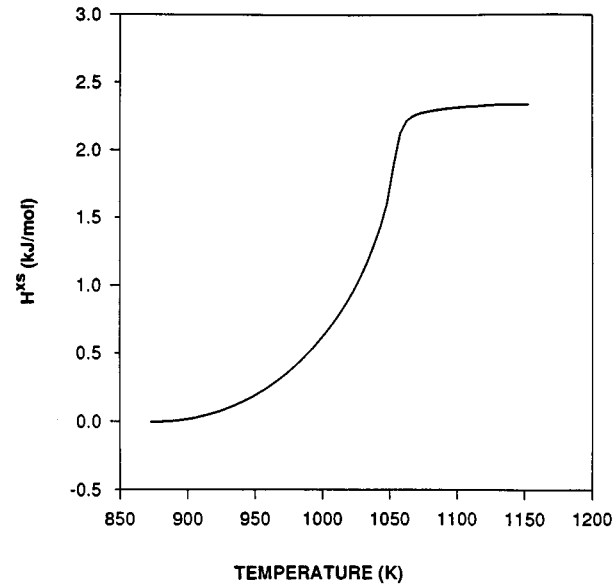

FIG. 2. Excess enthalpy vs temperature calculated by graphical integration of the area between the experimental C_p curve and the baseline.

of Eq. [4] to 298 K and integration:

$$H_T - H_{298} = R_{298} + \int_{298}^{T} C_p dT. \qquad [5]$$

The constant R_{298} has been obtained by the constraint, $H_T - H_{298} = 0$ for $T = 298$ K.

The resulting heat content is

$$H_T - H_{298} = -118836.633 - 22.7894T + 0.0420605T^2 + 5877.8382T^{0.5} + 608.2153 \times 10^4 T^{-1}. \qquad [6]$$

The enthalpy of transformation has been calculated by two procedures: (a) integration of the peak area under the C_p curve between 873 and 1153 K using the "linear" and "fitted" method from Netzsch program to define the baseline, and (b) graphical integration in the same temperature interval of the area between the experimental C_p curve and the baseline represented by a linear extrapolation of the C_p data between the two sides of the peak. The value calculated by both procedures was the same, 2.3 kJ/mol.

The transition enthalpy value depends on the width of the temperature interval considered for defining the baseline for integration. We chose the temperature interval based on the recent crystal structure study (13, 14) which shows that the anomalous variation of the unit cell dimensions of the orthorhombic $NaMgF_3$ perovskite started at 873 K. The excess enthalpy and excess entropy as functions of temperature obtained by graphical integration of the area between the experimental C_p curve and the baseline are presented in Figs. 2 and 3

$$\Delta H^{XS} = \int_{873}^{1153} C_p^{XS} dT$$

and

$$\Delta S^{XS} = \int_{873}^{1153} C_p^{XS}/T\, dT. \qquad [7]$$

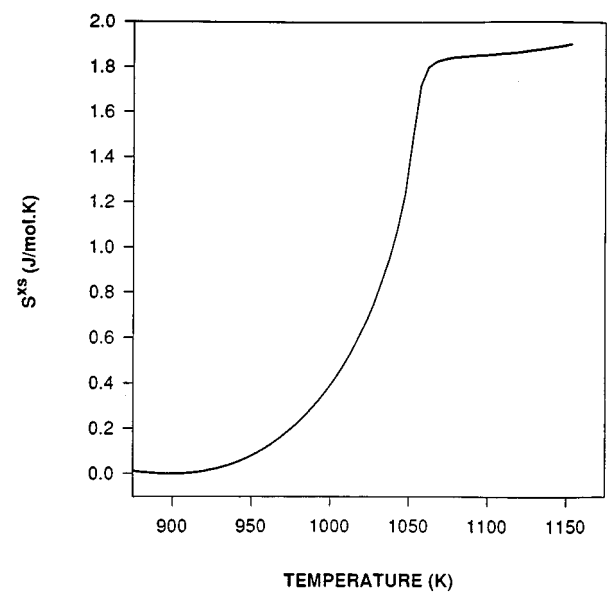

FIG. 3. Excess entropy vs temperature calculated by graphical integration of the area between the C_p/T curve and the baseline.

The tilting angle of MgF_6 octahedra in $NaMgF_3$ low-temperature phase is 15° (13) and is associated with a transition enthalpy of 2.3 ± 0.03 kJ/mol. This transition enthalpy value relative to the tilting angle is smaller than that measured in $A^{2+}B^{4+}O_3$ perovskites, for example, $CaTiO_3$ (10) and $SrZrO_3$ (12) with tilting angles of 10° and 6° have an enthalpy of transition of 6.5 and 2.0 kJ/mol, respectively. The smaller electrical charges associated with weaker ionic bonding in $NaMgF_3$ can account for this smaller value.

The heat content values have also been measured directly by transposed temperature drop calorimetry using the "hybrid" calorimeter. These experimental values together with those calculated by graphical integration of the experimental heat capacity data are presented in Fig. 4. There is excellent agreement between the two series of data, except for higher temperature interval after the transition where the average difference is about 3%. The larger difference at higher temperature may be explained by the increasing volatility of the $NaMgF_3$ with temperature. The higher volatility will affect the DSC values more due to the larger experimental time (1 h), compared with 12 min for heat content measurements or enthalpy of formation measurements. The experimental heat content data from Fig. 4 show a continuous variation with an inflection at around 1055 K corresponding to the transition temperature, which is in good agreement with 1051 K obtained by continuous heat capacity measurements as a function of temperature by DSC. Because the direct measurement of the heat capacities combined with structural data provides a more precise evaluation of the thermodynamic properties of the transition involving small energy than the differentiation of the integral experimental heat content values, we calculated the excess properties presented above using the direct DSC heat capacity data.

The phase transitions and structural distortion of perovskite can be viewed within Landau's phenomenological theory (29). In this mean-field approximation, the Gibbs free energy of the lower symmetry phase can be written in terms of the order parameter η,

$$G(P, T, \eta) = G_0(P, T) + a\eta^2 + b\eta^4 + c\eta^6 + \cdots, \quad [8]$$

where $G_0(P, T)$ is the Gibbs free energy of the high symmetry prototype and the excess Gibbs free energy of the low symmetry is represented by a power series with even terms in order parameter.

The order parameter η is related to the change in some macroscopic property through the phase transition and has a value of 0 in the high symmetry form and 1 in the low-symmetry form. The physical excess quantities and the structural parameters are highly correlated.

The spontaneous strain $\varepsilon^{(s)}$ for the m3mFmmm ferroelastic species, which describes the structural distortion of the crystal, has been identified to be the macroscopic order parameter of the phase transition from orthorhombic *Pbnm* to cubic *Pm3m* (14). A direct correlation then exists between the excess entropy ΔS^{XS} and the order parameter (30):

$$\Delta S^{XS} \propto \eta^2. \quad [9]$$

A plot of the spontaneous strain $\varepsilon^{(s)}$ versus the square root of the excess entropy is presented in Fig. 5 and shows a nonlinear dependence. We chose different values of C_p ideal (the baseline) to calculate the excess entropy. In the temperature

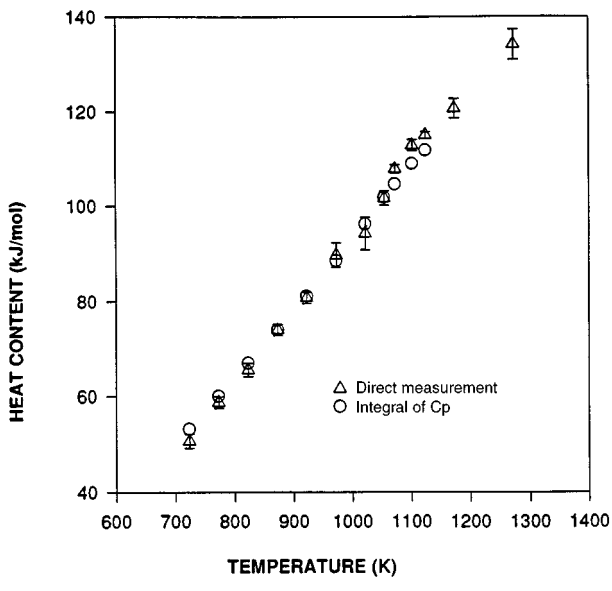

FIG. 4. Heat content ($H_T - H_{298}$) measured by transposed temperature drop calorimetry (triangles) and by graphical integration of the heat capacity data (circles).

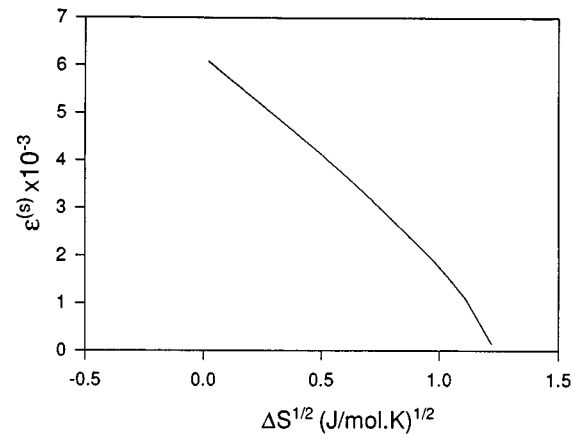

FIG. 5. Spontaneous strain vs square root of excess entropy.

interval considered in Fig. 5 (from 875 K to the transition temperature 1051 K) the excess entropy values did not change very much as a function of the subtracted baseline. The plot of the spontaneous strain versus the excess entropy calculated using different baselines shows deviation from linearity close to the transition temperature for all cases considered. This indicates that a single order parameter cannot completely account for the energetics of the transition. Coupling with other order parameters which have different temperature dependence may occur. The octahedral tilting angles may be considered another order parameter. A plot of the square of the tilting angles versus the square root of the excess entropy shows a similar nonlinear dependence. Thus neither spontaneous strain nor tilting angle functions as a single order parameter. Based on the X-ray study, two different types of structural deformation occur in the orthorhombic–cubic phase transition process (13): shrinkage of the octahedral (Mg–F) bond length and decrease of the MgF_6 octahedral tilting angles. These effects probably have different temperature dependences and different contributions to the thermal expansion and to the excess entropy.

The stability of the perovskite structure can be related to the A, B, and X ionic radii. A strict relation (tolerance factor of unity) between the relative sizes of the A and B ions would exist in an ideal cubic perovskite (31) where all ions contact in a close-packed structure. However, in real perovskites, the ionic radii do not simultaneously allow optimal AX and BX bond lengths. The size mismatch is eased by the displacement and oscillations of the ions from their cubic positions in different types of distorted perovskite structures. Kassen-Ogly and Naish (32) built a diagram of loose packing perovskite types using the relative values of ionic radii from Shannon's tables (33) (considering the valency and coordination number). In this diagram $NaMgF_3$ is the only fluoride in the $AMgF_3$ series (A = Na, K, Rb) in which a phase transition occurs by tilting the MgF_6 octahedra. This is in agreement with the X-ray diffraction study (6, 13, 14).

Recently a theromodynamic study of ABF_3 type fluoperovskites (A = K, Rb, Cs) (B = Cd, Ca) was carried out. (34–36). Structural phase transitions at different temperatures (between 10 and 560 K) have been identified for all except $CsCaF_3$ and $CsCdF_3$. The stability of the fluoperovskite structure was correlated with the ionic radii. A phase transition due to the rotation of the BF_6 octahedra may occur when the lattice parameter a is greater than $(r_A^+ + r_F^-)\cdot\sqrt{2}$ (37). The B ions in the ABF_3 compounds studied are large enough to have a lattice parameter which satisfies this condition except for $CsBF_3$. The lower temperatures seen for these rotational transitions compared to the tilting transition suggests that the former are probably associated with much smaller energies, probably <1 kJ/mol.

CONCLUSIONS

The enthalpy of formation $NaMgF_3$ has been obtained directly without correction for heat content or heat of fusion, by a new methodology. The heat capacity measured between 313 and 1153 K shows a λ-anomaly which has been correlated with a phase transition. Previous X-ray study indicates a sequence of phase transitions from orthorhombic to tetragonal to cubic. The present results support the recent X-ray study which shows that the crystal structure transforms from the orthorhombic *Pbnm* phase directly to the cubic *Pm3m* phase. The excess thermodynamic properties have been calculated and correlated with the order parameter. A plot of spontaneous strain versus the square root of the excess entropy shows a nonlinear dependence. This non-Landau behavior can be explained by coupling between more than one order parameter. The heat content values measured directly are in good agreement with those calculated by integration of heat capacity data and show only one inflection corresponding to one phase transition.

ACKNOWLEDGMENT

This research was supported by the Center for High Pressure Research, (CHiPR), an NSF Science and Technology Center.

REFERENCES

1. R. Jeanloz and A. B. Thompson, *Rev. Geophys. Earth Phys.* **21,** 51 (1983).
2. A. Navrotsky and D. J. Weidner, "Perovskite: A Structure of Great Interest to Geophysics and Materials Science," p. 67. American Geophysical Union, Washington, DC, 1989.
3. A. K. Misra and J. D. Whittenberger, *Proc. Intersociety Energy Conversion Engineering Conference* **1,** 188 (1987).
4. A. K. Misra, *J. Electrochem. Soc.* **135,** 850 (1988).
5. Y. Takahashi, A. Negishi, Y. Abe, K. Tanaka, and M. Kamimoto, *Thermochim. Acta* **183,** 299 (1991).
6. E. C. T. Chao, H. T. Evans, B. J. Skinner, and C. Milton, *Am. Miner.* **46,** 379 (1961).
7. M. Marezio, J. P. Remeika, and P. D. Dernier, *Acta Crystallogr. B* **26,** 2008 (1970).
8. M. O'Keeffe, B. G. Hyde, and J.-O. Bovin, *Phys. Chem. Miner.* **4,** 299 (1979).
9. X. Liu and R. C. Liebermann, *Phys. Chem. Miner.* **20,** 171 (1993).
10. F. Guyot, P. Richet, P. Courtial, and P. Gillet, *Phys. Chem. Miner.* **20,** 141 (1993).
11. Y. Zhao and D. J. Weidner, *Phys. Chem. Miner.* **18,** 294 (1991).
12. D. de Ligny and P. Richet, *Phys. Rev. B* **53,** 3013 (1996).
13. Y. Zhao, D. J. Weidner, J. B. Parise, and D. E. Cox, *Phys. Earth Planet. Interiors* **76,** 1 (1993).
14. Y. Zhao, D. J. Weidner, J. B. Parise, and D. E. Cox, *Phys. Earth Planet. Interiors* **76,** 17 (1993).
15. National Bureau of Standards Certificate, "Synthetic Sapphire (α-Al_2O_3)." Standard Reference Material 720, April 1982.
16. L. Topor and A. Navrotsky, "Application to Earth and Planetary Sciences," p. 71. Terra Scientific (1992).
17. W. G. Jung, O. J. Kleppa, and L. Topor, *J. Alloys Compounds* **176,** 309 (1991).

18. J. C. Gachon, *J. Phys. Chem. Solids* **49,** 435 (1988).
19. A. Navrotsky, *Phys. Chem. Miner.* **2,** 89 (1977).
20. H. R. Westrich and A. Navrotsky, *Am. J. Sci.* **281,** 1091 (1981).
21. J. L. Holm, B. J. Holm, and M. Rotnes, *Acta Chem. Scand.* **26,** 1687 (1972).
22. S. H. Elder, F. J. DiSalvo, L. Topor, and A. Navrotsky, *Chem. Mater.* **5,** 1545 (1993).
23. O. K. Sokolov and A. J. Belyaev, *Izv. Vysshikh. Uchebn. Zavednii. Tsvetn. Met.* **3,** 72 (1960).
24. K. C. Hong and O. J. Kleppa, *J. Phys. Chem.* **82,** 1596 (1978).
25. R. Robie, B. S. Hemingway, and J. R. Fisher, "Thermodynamic Properties of Minerals and Related Substances at 298.15 K and 1 Bar (10^5 Pascals) Pressure and at Higher Temperatures," p. 292. U.S. Government Printing Office, Washington, DC, 1979.
26. J. L. Haas, Jr., and J. R. Fisher, *Am. J. Sci.* **276,** 525 (1976).
27. P. Richet and G. Figuet, *J. Geophys. Res.* **96,** 445 (1991).
28. P. Richet, R. A. Robie, J. Rogez, B. S. Hemingway, P. Courtial, and C. Téqui, *Phys. Chem. Miner.* **17,** 385 (1990).
29. L. D. Landau and E. M. Lifshitz, "Statistical Physics," 2nd ed. Pergamon, Oxford, 1969.
30. E. Salje, *Ferroelectrics* **104,** 111 (1990).
31. A. Putnis, "Introduction to Mineral Sciences," p. 137. Cambridge Univ. Press, Cambridge, UK, 1992.
32. F. A. Kassan-Ogly and V. E. Naish, *Acta Crystallogr. B* **42,** 307 (1986).
33. R. D. Shannon, *Acta Crystallogr. A* **32,** 751 (1976).
34. F. Koussinsa, B. Bonnetot, and M.Diot, *Thermochim. Acta* **206,** 1 (1992).
35. F. Koussinsa and M. Diot, *Thermochim. Acta* **216,** 87 (1993).
36. F. Koussinsa and M. Diot, *Thermochim. Acta* **216,** 95 (1993).
37. M. Rousseau, J. Y. Gesland, J. Julliard, and J. Nouet, *Phys. Rev. B* **12,** 1579 (1975).
38. A. Navrotsky, *Phys. Chem. Miner.* **24,** 222 (1997).